

Kinetic Modelling of Divertor Fluxes during ELMs in ITER and Effect of In/Out Divertor Plasma Asymmetries^{*)}

Masanari HOSOKAWA, Alberto LOARTE, Guido T.A. HUIJSMANS,
Tomonori TAKIZUKA¹⁾ and Nobuhiko HAYASHI²⁾

ITER Organisation, Route de Vinon sur Verdon, CS 90 046, 13067 St Paul Lez Durance Cedex, France

¹⁾*Graduate School of Engineering, Osaka University, Suita, Osaka 565-0871, Japan*

²⁾*National Institutes for Quantum and Radiological Science and Technology, Naka, Ibaraki 311-0193 Japan*

(Received 21 April 2016 / Accepted 14 June 2016)

Particle and energy fluxes to the plasma facing components (PFCs) during edge localized modes (ELMs) are expected to unacceptably shorten the PFCs lifetime in ITER. In order to understand the consequences of kinetic effects of ELMs to PFCs, PARASOL simulations have been carried. Initial 1-D simulations showed that both the in/out asymmetry of divertor parameters before ELMs as well as the magnitude of the ELM energy loss itself have an influence on the in/out asymmetry of the ELM divertor fluxes with the total energy deposited at the divertor being larger at the hotter/lower recycling divertor. The role of the thermoelectric current (I_{SOL}) has been studied with further 1-D simulations in which decreasing I_{SOL} leads to an increase of the ELM power deposition at the colder/higher recycling divertor but the degree of in/out asymmetry is smaller than in the experiment. PARASOL-2D simulations have been carried out to study the effects of plasma drifts on the asymmetries of ELM energy and particle transport. It shows that for the favourable ∇B direction the ELM energy flux is predominantly deposited at the inner divertor while for the unfavourable ∇B direction it is at the outer divertor, which is in agreement with experimental findings.

© 2016 The Japan Society of Plasma Science and Nuclear Fusion Research

Keywords: scrape-off layer, divertor plasma, particle-in-cell simulation, edge localized mode, thermoelectric current

DOI: 10.1585/pfr.11.1403104

1. Introduction

Particle and energy fluxes to the plasma facing components (PFCs) during uncontrolled edge localized modes (ELMs) are expected to unacceptably shorten the PFC lifetime for high Q scenarios in ITER on the basis of empirical extrapolations from existing experiments [1]. Non-linear MHD modelling of these particle and energy fluxes carried out for ITER has shown that some aspects of such empirical extrapolations, such as the scaling of the broadening of the ELM power footprint at the divertor with ELM energy loss, may not apply at the ITER scale [2]. However, the robustness of these findings is questionable because the particle and energy transport along the field lines in these MHD simulations are modelled in a fluid approximation. This is not applicable during an ELM in ITER because this transport is essentially collisionless given the high plasma temperatures in the pedestal plasma. In order to understand the consequences of kinetic effects on ELM energy and particle transport, modelling of typical edge plasma conditions during (and between) ELMs in ITER has been carried out with the PARASOL (PARTicle Advanced simulation for SOL and divertor plasmas) particle-in-cell code in

1-D and 2-D approximations [3]. Initial simulations with PARASOL 1-D [4] had shown that both the in/out asymmetry of divertor parameters between ELMs (due to different recycling conditions at the two divertors) as well as the magnitude of the ELM energy loss itself have an influence on the in/out asymmetry of the ELM divertor power fluxes, although the total energy deposited by the ELM tends to be biased towards the divertor with lower recycling between ELMs (outer divertor for the ∇B direction favourable for H-mode access), which is contrary to experimental observations. This was identified to be due to the fact that large thermoelectric currents circulate between the two divertors during the ELMs in the simulations. Although at the inner divertor the product of ion flux and plasma temperature ($T_e + T_i$) during the ELM is largest (due to the higher recycling), the sheath transmission coefficient at the outer divertor is typically a factor of 2-8 times higher than at the inner divertor during the ELM, due to the strong thermoelectric currents, which leads to the ELM power flux at the outer divertor to be largest [4]. To understand the role of thermoelectric currents on ELM power deposition asymmetries, PARASOL 1-D simulations have been carried out where one divertor target (the inner one, higher recycling between ELMs) is assumed to be floating so that thermoelectric current flow during ELMs is considerably reduced,

author's e-mail: masanari.hosokawa@iter.org

^{*)} This article is from 15th International Workshop on Plasma Edge Theory in Fusion Devices.

Table 1 Modelling parameters for ITER simulations in PARASOL 1-D between ELMs and at the ELMs.

Toroidal magnetic field (T)	5.3	Hot source region	$0.24L \sim 0.76L$
Major/Minor radius (m)	6.2/2.0	Pitch angle	0.25
Poloidal length L (m)	33	Recycling temp. (eV)	2.5
SOL width (m)	0.02	Recycling Ratio “in/out”	0.5/0.0, 0.99/0.0
Mass ratio m_i/m_e	3670	ELM temp. (keV)	1.0, 2.5, 5.0
Separatrix density (m^{-3})	1.0×10^{20}	ELM duration τ_{ELM} (μs)	200
Separatrix temp. (eV)	300	ELM width L_{ELM}	$0.27L$
Z_{eff}	1.5		

which is found to affect the in/out ELM divertor power flux asymmetry in the direction expected, as described in Sec. 3.

The PARASOL 2-D code was previously used for the modelling of kinetic effects on the SOL flow pattern for stationary plasmas including plasma drifts [3, 5]. This has been further extended to include ELMs by the development of a simple ELM model in PARASOL 2-D. We have considered two magnetic configurations for plasmas in a single null poloidally diverted geometry: one with the favourable ion ∇B drift direction for H-mode access (so called “normal” ∇B) and the other with unfavourable ion ∇B drift direction for H-mode access (so called “reversed” ∇B). In these 2-D simulations other effects that introduce in/out divertor asymmetries between ELMs, associated with impurity radiation, different divertor recycling conditions, etc., are not yet included.

In the next section, the simulation models and parameters of the PARASOL 1-D and 2-D codes are described. Simulation results are presented in Sec. 3, and Sec. 4 consists of a summary of the results and required further work. Additional previous studies with PARASOL 1-D and 2-D can be found in [6–9]. Kinetic modelling for the SOL plasma between and during ELMs in existing fusion devices and ITER with other PIC codes are described in [10–13].

2. Simulation Models and Parameters

2.1 1-D ELM simulation with floating divertor

The 1-D SOL-divertor plasma simulated by the PARASOL code [3] is bounded by two divertor plates located at $x = 0.0$ and 1.0 , where the x direction corresponds to the poloidal direction for the SOL-divertor region in a tokamak. We consider a plasma with one species of singly charged ions (mass m_i and charge e) and electrons (mass m_e and charge $-e$), for simplicity. The orbits of ions are fully traced, while guiding-centre orbits are followed for electrons. The anomalous transport is simulated with a Monte-Carlo random-walk model. The effects of Coulomb collisions are simulated by using a binary collision model [6]. The electric field $E_x = -\partial\phi/\partial x$ is determined by Pois-

son’s equation (Eq. (1)). Ion and electron densities, n_i and n_e , are calculated self-consistently with the PIC method of the area-weighting scheme. The magnetic field \mathbf{B} is taken to be constant in the SOL-divertor with a pitch of $\Theta = B_x/B$, whose value is set 0.25 in this study and intersects the divertor plates obliquely. Table 1 shows the modelling parameters of the ITER simulations for plasma conditions between the ELMs and during the ELMs. The value of the separatrix density (10^{20} m^{-3}) has been chosen artificially high to obtain very asymmetric plasma conditions between the two divertor plasmas with PARASOL to study the effect of divertor asymmetries between ELMs on the particle and power asymmetries during the ELMs. This density value was required because the recycling and radiative losses modelled in PARASOL are simplified compared to those in 2-D fluid simulation codes [14]. The inter-ELM plasma conditions between the two divertors were varied by adjusting the recycling coefficient R_{rec} for the particle and radiative losses so that the inner divertor was colder and denser than the outer one which is in agreement with experimental observations for “normal” ∇B . Two levels have been studied Mid-recycling $R_{\text{rec}} = 0.5$ and High recycling $R_{\text{rec}} = 0.99$. In this paper we show the results for High recycling only, the reader is referred to [4] where the High recycling and Mid-recycling cases were compared. The choice of 0.99/0.0 in/out divertor recycling levels represents an example of an extreme asymmetry in/out divertor recycling asymmetry. The level of 0.99 is typical of divertor conditions in ITER over a large density range, i.e. the core ionization source due to neutral escape from the divertor is typically less than 1% of the divertor ion flux in ITER [15]. The ELMs are modelled by the addition of a number of particles (N_{ELM}) with a temperature (T_{ELM}) in the SOL for a time interval (τ_{ELM}) where the values of these parameters are adjusted to reproduce the expectations for ITER [1].

The electrostatic potential ϕ is determined by the one dimensional Poisson’s equation as

$$-\partial^2\phi/\partial x^2 = (e/\epsilon_0)(n_i - n_e), \quad (1)$$

where ϵ_0 is the permittivity of vacuum. In the simulations we model the (inner) floating divertor by applying a difference of electric potential $\Delta\phi$ ($\phi_{\text{in}} = \Delta\phi, \phi_{\text{out}} = 0$) be-

tween the two divertors as boundary condition. The SOL-averaged electric current J_x is thus given by

$$J_x = eL^{-1} \int dx (\langle n_i v_{xi} \rangle - \langle n_e v_{xe} \rangle) / N_{av}, \quad (2)$$

where $v_{xi,xe}$ are the velocities of the charged particles and N_{av} is the SOL-averaged ion density. To reduce the thermoelectric current a potential difference $\Delta\phi$ is applied at the inner divertor to obtain

$$\Delta\phi = C_v \int_{\Delta t} dt (J_x - J_0), \quad (3)$$

where the input parameters on the strength of floating potential C_v and the desired thermoelectric current J_0 are adjusted from the modelling results between ELMs by imposing $C_v = 0.1$, $J_0 = 0$ and are kept constant between the ELMs and during the ELMs in order to get the thermoelectric currents reduced during the ELMs, while $\Delta\phi$ is varied in time. $\Delta\phi$ in Eq. (3) is integrated over the interval Δt , which is the time-step used in this modelling.

2.2 2-D ELM simulations on opposite X-point positions

The tokamak plasma is simulated in a cylindrical coordinate system (r, θ, z) inside a rectangular region in the r - z plane surrounded by rectangular walls, $-a_w < r - R_0 < a_w$ and $-b_w < z < b_w$, where R_0 is the major radius of the vessel centre (Fig. 1). A regular rectangular grid is adopted for the PIC modelling and axisymmetry is assumed. The magnetic field for the poloidally diverted configurations considered $B = (B_r, B_\theta, B_z)$ is produced by the combination

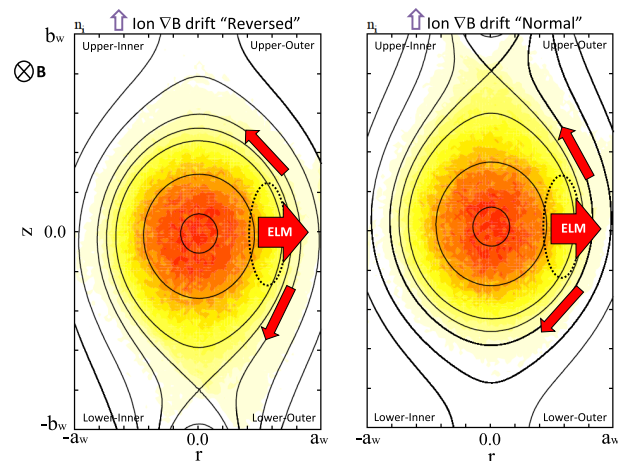


Fig. 1 Modelling geometries for the PARASOL 2-D in cylindrical coordinates (r, θ, z) for lower & upper single null configuration (LSN and USN respectively) illustrating the ∇B drift direction. The left hand side figure shows the LSN case in which the ion ∇B drift is towards opposite to the active X-point (i.e. "reversed" ∇B) and the right hand side figures is for the USN case in which the ion ∇B drift is towards to active X-point (i.e. "normal" ∇B).

of a core plasma current channel and two divertor coil currents. The plasma minor radius a is defined at the midplane separatrix, and the aspect ratio is given as $A \equiv R_0/a$. The toroidal magnetic field B_θ is proportional to $1/R$, and the pitch of magnetic field $\Theta \equiv |B_z/B_\theta|$ is provided at the outer mid-plane separatrix as input parameter. The orbits of ions are fully traced and solved with the leap-frog method, while guiding-centre orbits are followed for electrons by using the predictor-corrector method. Poisson's equation in the two dimensional cylindrical coordinates is approximated by the finite difference equation, and is solved by the tri-diagonal matrix algorithm (TDMA) in the r direction and the fast Fourier transform (FFT) algorithm in the z direction. The electrostatic potential, including the sheath potential at the plasma-wall boundary, is fully simulated. The rectangular wall boundary is considered to be electrically conductive, and the wall potential is set $\phi = 0$. A source of hot particles is injected in the core plasma to simulate plasma heating. In this study, a uniform source of hot particle is considered for the core plasma region inside the magnetic separatrix ($-a < r < a$ at the midplane). Ions and electrons with a temperature $T_{i0} = T_{e0} = T_0$ are supplied uniformly in this region with hot ion and electron pairs being born at the same spatial position.

The number of ions in the simulations N_i is 10^6 and the number of spatial cells $M_R \times M_z$ is 320×512 and the size of each cell is 0.25 both for r and z direction and the normalized length is determined as $\Delta l = \Delta t * v_{th,e}$, where Δt is the normalized time-step and $v_{th,e}$ is the electron thermal velocity. The mass ratio m_i/m_e is chosen as 400 to save computation time. The aspect ratio A is set as 5.4 and the pitch of the magnetic field Θ is 0.2 at the outer mid-plane separatrix determining the parallel connection length $L_{||} \sim 2\pi a/\Theta$. The typical ratio of the ion Larmor radius to plasma minor radius in these simulations is $\rho_{i0}/a = 0.02$ (ρ_{i0} : ion Larmor radius at hot ion temperature T_{i0} , a : plasma minor radius) and various values of plasma $L_{||}/\lambda_{mfp}$ have been considered from collisionless to collisional plasmas, where λ_{mfp} is the electron-electron collisional mean free path. Regarding the ELM parameters, two normalized ELM durations have been considered $\tau_{ELM}/\tau_{||,i} = 0.16$ (short) and 2 (long) where $\tau_{||,i}$ is the SOL parallel ion transit time $\tau_{||,i} \sim L_{||}/C_s$ (C_s is sound speed). The resulting ELM energy losses for the main plasma are very small $\Delta W/W_{sep} < 1\%$, as required for controlled ELMs in ITER [1]. It should be noted that, due the scaling of the ratio of plasma drift velocities to the sound speed with the size of the modelled system, the effects of drifts in our simulations (which have a much smaller size than the real plasma) are augmented with respect to the experiment [13] and thus only the relative (not quantitative) effects of drifts can be modelled with our approach.

The anomalous transport is simulated with a Monte-Carlo random-walk model. A spatial displacement perpendicular to B , Δr_{anom} , is added for every time step in the motion equations both on electrons and ions. The isotropic

displacement is given by a Gaussian random number g , and its mean square is

$$\langle \Delta \mathbf{r}_{\text{anom}}^2 \rangle = D_{\text{anom}} \Delta t, \quad (4)$$

$$\delta \mathbf{v}_{\perp} = \Delta \mathbf{r}_{\text{anom}} / \Delta t = (D_{\text{anom}} / \Delta t)^{0.5} g. \quad (5)$$

The ELM modelling in this study is implemented by multiplying Eq. (5) by a constant k_{ELM} in a selected region of the plasma and added as an additional displacement caused by the ELM to both electrons and ions to simulate the expulsion of particles by the ELM. The parameters chosen in the cases $\tau_{\text{ELM}} / \tau_{\parallel, i} = 0.16$ (short) and 2 (long) are $k_{\text{ELM}} = 0.5$ and 0.05 respectively. The region over which k_{ELM} is introduced leads to particles entering SOL in the outer midplane region as shown in Fig. 1.

3. Simulation Results

3.1 Effect of thermal electric currents on ELM in/out deposition asymmetries

Figure 2 shows the time evolution of particle flux Γ_x and thermoelectric SOL current (I_{SOL}) for a Type-I ELM with total energy $E_{\text{ELM}} = 20$ MJ and $T_{\text{ELM}} = 5$ keV for ITER for in/out asymmetric divertor plasma conditions between ELMs ($n_{\text{in}} = 3.1 \times 10^{21} \text{ m}^{-3}$, $T_{\text{in}} = 1.5$ eV and $n_{\text{out}} = 2.7 \times 10^{19} \text{ m}^{-3}$, $T_{\text{out}} \sim 100$ eV, in/out recycling ratio 0.99/0.0). Figures 2(a) and 2(b) are results with fixed potential boundary condition that allow thermoelectric current flow ($\phi_{\text{in}} = \phi_{\text{out}} = 0$), and Figs. 2(c) and 2(d) are for the case in which the inner divertor is floating ($\phi_{\text{in}} = \Delta\phi$, $\phi_{\text{out}} = 0$). The simulations allowing thermoelectric current I_{SOL} showed [4] that the particle flux is

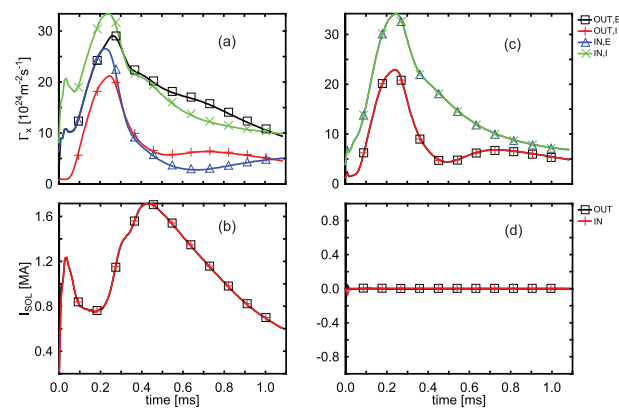


Fig. 2 Time evolution of (a) particle flux and (b) thermoelectric current on the inner/outer divertors with fixed boundary conditions ($\phi_{\text{in}} = \phi_{\text{out}} = 0$). (c) and (d) correspond to the particle flux and thermoelectric current in case of floating inner divertor. When the inner divertor is floating the thermoelectric current I_{SOL} is significantly decreased. Reducing I_{SOL} increases the ELM power and energy flux to the inner divertor as electron particle flux increases to the same value of the ion flux which is largest at the inner divertor. The increased influx of high energy particles into the 1-D SOL associated with the ELM starts at $t = 0$.

higher at the inner divertor before the ELM and increases faster when the ELM starts leading to a larger power being initially deposited at the inner divertor (in the ion channel). However, at the time of the peak power deposition both inner and outer power fluxes are similar and, correspondingly, the total heat load deposited in the two divertors by the ELM. In agreement with previous simulations the largest fraction of the ELM energy is deposited by ions [3, 10, 11]. Because of the asymmetry of the temperature between ELMs at the divertor, I_{SOL} appears between the inner and the outer divertor (Fig. 2 (b)) and this leads to more electrons reaching the outer divertor target (Fig. 2 (a)) and to a larger electron heat flux there. This compensates the initial asymmetry caused by the ion flux and leads to an overall symmetric ELM energy deposition at the two divertors when I_{SOL} flows in the SOL. When the boundary condition is modified so that the inner divertor is floating the electron & ion particle fluxes are similar on both divertors (Fig. 2 (c)) whilst the value of the ion fluxes at the two divertors remain as in the case with I_{SOL} . This leads to a higher power flux to be deposited at the higher recycling divertor in agreement with the high ion flux there as is in this case electron and ion fluxes at each of the two divertors is the same due to the absence of net SOL current. It should be noted that, while these simulations include the effect of in/out divertor recycling asymmetries leading to different ion fluxes and neutrals densities at the two divertors during the ELM, they do not include the effect of charge-exchange (CX) between the outflowing ions with the incoming neutrals which have been found to be important in other studies [12]. A model for CX implemented in PARASOL is being presently in the process of verification to enable us to assess the effects of CX in our simulations.

The ratio of asymmetric inner/outer divertor ELM energy deposition (Fig. 3 (top)) and power flux deposition (Fig. 3 (bottom)) shows that the effects of thermoelectric current are to increase the balance towards the inner divertor. The magnitude of the effect is larger for the ELM power flux asymmetry than for the ELM energy flux asymmetry and for the latter the larger effects are found for smaller energy losses $\Delta W_{\text{ELM},0}$. The level of in/out ELM power flux deposition asymmetry can be as high as 4 but, the in/out ELM energy deposition asymmetry typically obtained is not larger than 1.2 and thus lower than the factor of 2 typically found in experiment. In these simulations we have considered various combinations of the energy and quantity of ions/electrons expelled into the SOL by the main plasma during the ELM which correspond to the same total ELM energy loss ΔW_{ELM} . The range covers an electron/ion temperature of 5 keV (expected pedestal temperature in ITER for $Q = 10$ operation [2]) to 1 keV. Correspondingly, the total number of electrons/ions expelled by the ELM has been adjusted to obtain the same ΔW_{ELM} for all the ELM-expelled ion/electron temperatures. This reproduces, in a simplified way, the well-established experimental observation that, depending on plasma conditions,

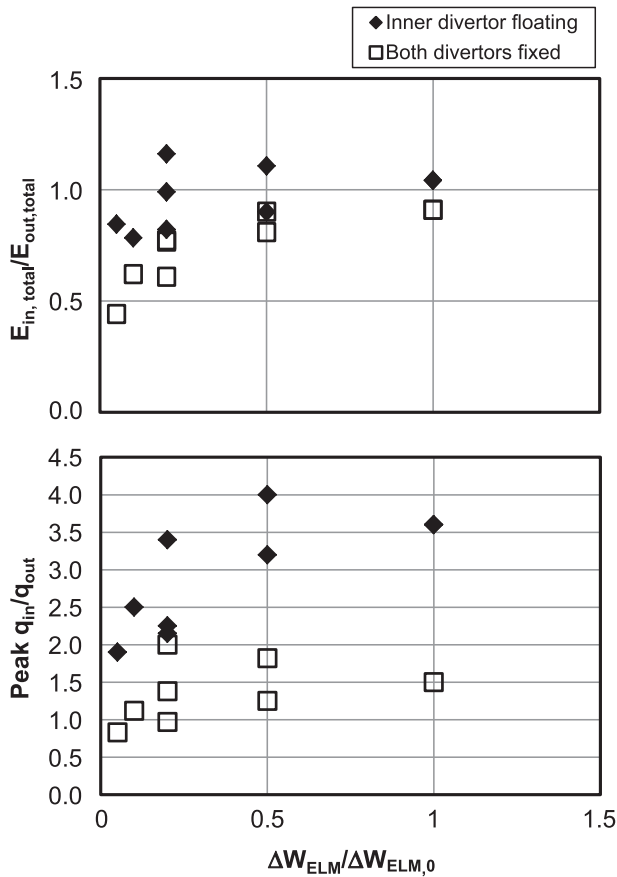


Fig. 3 Level of asymmetry in ELM energy deposition E_{in}/E_{out} (top) and in the peak ELM power flux q_{in}/q_{out} (bottom) as a function of normalized ELM energy $\Delta W_{ELM}/\Delta W_{ELM,0}$, where $\Delta W_{ELM,0}$ corresponds to the uncontrolled ITER ELM energy loss of 20 MJ. Both the asymmetries increase with reduced thermoelectric SOL current I_{SOL} (solid points correspond to an inner floating divertor with reduced I_{SOL} and open points correspond to the cases with $\phi_{in} = \phi_{out}$ with large I_{SOL}).

ELM energy losses can be dominated by plasma conduction (loss of fewer and more energetic ions/electrons) or convection (loss of a larger number of particles of lower energy) [16].

3.2 Asymmetric heat load dependence on ion ∇B drift direction

Figure 4 shows the time evolution of the modelled power (top) and energy (bottom) fluxes at the inner and outer divertors during an ELM modelled with PARASOL-2D. Figures 4 (a)-(b) correspond to the case which the ion ∇B drift direction is “reversed” and Figs 4 (c)-(d) correspond to the “normal” ion ∇B direction. The time τ_{e1} is the time at which the electron power flux is highest at the outer target and τ_{e2} is the one for the inner target. τ_{i1} is the time when the ion heat power flux is highest at the outer target and τ_{i2} is the same for the inner target case. A fast-time-scale transient behaviour is observed in the electron flux q_e

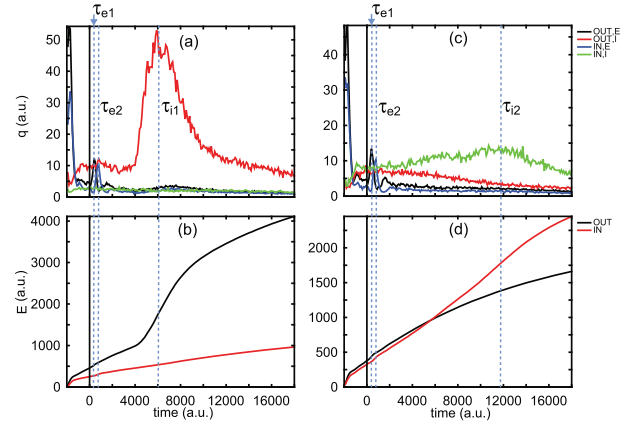


Fig. 4 Transient responses of (a) heat flux (q) and (b) energy deposition (E) for the “reversed” ion ∇B drift direction. (c) and (d) correspond to the case of “normal” ion ∇B drift direction. The time τ_{e1} is the one when electron heat flux at outer target is peaked, τ_{e2} is the time when electron heat flux at inner target is peaked. τ_{i1} is the one when ion heat flux is peaked for the “reversed” ∇B case, τ_{i2} is for the “normal” ∇B case. In/out energy load asymmetries are strongly affected by ion ∇B drift direction. The energy deposition asymmetry E_{in}/E_{out} is ~ 0.3 for the case of ∇B “reversed”, while E_{in}/E_{out} is ~ 1.5 for the case of “normal” ∇B . The increase in edge transport coefficients which leads to the outflux of high energy particles from the edge plasma into the 2-D SOL associated with the ELM starts at $t = 0$. The ELMs simulations were restarted from two steady states. The lack of complete information in the re-start files (for practical reasons) leads to some parameters having default values when the simulation is restarted and to a fast (\sim electron transit time) re-arrangement of the electron population that leads to the peaks in the electron heat fluxes at the inner and outer divertor at $t = -2000$. These are of no consequence for the rest of the ELM simulation that starts at $t = 0$ and takes place in ion transit time scales.

for both ion ∇B drift directions, $\tau_{e1} \sim \tau_{ELM}$ at outer target and $\tau_{e2} \sim 2\tau_{ELM}$ at inner target which is determined by the ELM particle expulsions geometry losses concentrated at the outer midplane closest to the outer target. The slow-time-scale transient behaviour observed in the ion power flux, on the contrary, depends strongly on the direction of the ∇B drift: $\tau_{i1} \sim 15\tau_{ELM} \sim 2.4\tau_{\parallel,i}$ for the “reversed” ∇B and $\tau_{i2} \sim 30\tau_{ELM} \sim 4.8\tau_{\parallel,i}$ for the “normal” ∇B drift directions.

Figure 5 presents the time evolution of the power flux asymmetry q_{in}/q_{out} in PARASOL 2-D runs for the two ion ∇B directions with a minimum $q_{in}/q_{out} \sim 0.2$ at τ_{i1} for the “reversed” ∇B case and $q_{in}/q_{out} \sim 2.7$ at τ_{i2} for the “normal” ∇B case. The resultant ELM energy deposition asymmetry is $E_{in}/E_{out} \sim 0.3$ for “reversed” ∇B case and $E_{in}/E_{out} \sim 1.5$ for “normal” ∇B case. These trends are qualitatively consistent with experimental findings of $E_{in}/E_{out} \sim 1.0 - 2.0$ for “normal” ∇B case $E_{in}/E_{out} \sim 0.5 - 1.0$ for “reversed” ∇B [17].

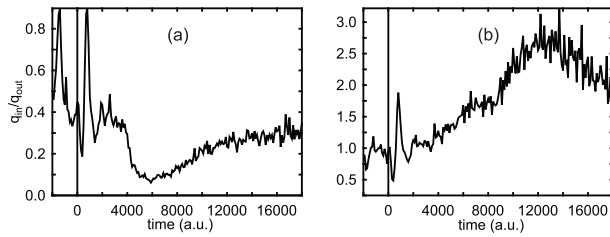


Fig. 5 Time evolution of the ELM power heat flux in/out divertor asymmetry for: (a) “reversed” ∇B and (b) “normal” ∇B . The in/out ELM power flux asymmetry changes drastically with the ion ∇B drift direction. The in/out asymmetry q_{in}/q_{out} is ~ 0.1 for “reversed” ∇B and q_{in}/q_{out} is ~ 2.7 for “normal” ∇B .

4. Summary and Further Work

The effects of divertor recycling and thermoelectric currents on the in/out divertor ELM power flux load asymmetries have been modelled with PARASOL 1-D, and the effect of the ∇B direction on divertor ELM power flux asymmetries in 2-D magnetic configurations has been modelled with PARASOL 2-D. Thermoelectric currents have a strong influence on the ELM power flux asymmetry and enhance the ELM power flux load at the divertor which is hotter/lower recycling between ELMs. Reducing thermoelectric currents increases the ELM power flux at the divertor which is colder/higher recycling between ELMs but the power flux/energy load in/out asymmetry during ELMs remains lower than the usual factor of 2 found in experiments for the “normal” ∇B direction in which the inner divertor is colder/higher recycling than the outer one between ELMs. The direction of ion ∇B drift direction has a very strong effect on the ELM heat power flux in/out divertor asymmetry with deposition to the inner divertor being dominant for “normal” ∇B and to the outer divertor for “reversed” ∇B . This is robust to modelling assumptions (ELM duration and plasma collisionality) and

in qualitative agreement with experimental measurements. The complete picture including the direct effects of the ∇B direction during ELMs and the effects of the ∇B direction on in/out divertor asymmetries between ELMs requires inclusion of a recycling model in PARASOL-2D, which is progress.

Acknowledgments

The views and opinions expressed herein do not necessarily reflect those of the ITER Organization. ITER is the Nuclear Facility INB no. 174.

©2016 ITER

- [1] A. Loarte *et al.*, Nucl. Fusion **54**, 033007 (2014).
- [2] G.T.A. Huijsmans and A. Loarte, Nucl. Fusion **53**, 123023 (2013).
- [3] T. Takizuka, Plasma Sci. Technol. **13**, 316 (2011).
- [4] M. Hosokawa, A. Loarte, G.T.A. Huijsmans, T. Takizuka and N. Hayashi, Proc. 41st EPS Conf., paper P5.003 (Berlin, Germany, 2014).
- [5] T. Takizuka, K. Shimizu, N. Hayashi, M. Hosokawa and M. Yagi, Nucl. Fusion **49**, 075038 (2009).
- [6] T. Takizuka and H. Abe, J. Comput. Phys. **25**, 205 (1977).
- [7] T. Takizuka and M. Hosokawa, Contrib. Plasma Phys. **46**, 698 (2006).
- [8] T. Takizuka and M. Hosokawa, Trans. Fusion Sci. Technol. **51**, 271 (2007).
- [9] T. Takizuka, N. Oyama and M. Hosokawa, Contrib. Plasma Phys. **48**, 207 (2008).
- [10] D. Tskhakaya *et al.*, J. Nucl. Mater. **390-391**, 335 (2009).
- [11] R.A. Pitts *et al.*, Nucl. Fusion **47**, 1437 (2007).
- [12] D. Tskhakaya *et al.*, J. Nucl. Mater. **415**, S860 (2011).
- [13] D. Tskhakaya *et al.*, Theory of Fusion Plasmas, Societa Italiana di Fisica, Bologna, Italy, 97 (2004).
- [14] A.S. Kukushkin *et al.*, Nucl. Fusion **49**, 075008 (2009).
- [15] A. Loarte *et al.*, J. Nucl. Mater. **401-405**, 463 (2015).
- [16] A. Loarte *et al.*, Plasma Phys. Control. Fusion **44**, 1815 (2002).
- [17] T. Eich *et al.*, J. Nucl. Mater. **363-365**, 989 (2007).